

Quantum Walks with Entangled Coins

S. E. Venegas-Andraca,¹ J. L. Ball,¹ K. Burnett,¹ and S. Bose²

¹*Centre for Quantum Computation, Clarendon Laboratory,
University of Oxford, Parks Road, Oxford OX1 3PU, United Kingdom*

²*Department of Physics and Astronomy, University College of London. Gower Street, London WC1E 6BT, United Kingdom.*

We present a mathematical formalism for the description of unrestricted quantum walks with entangled coins and one walker. The numerical behaviour of such walks is examined when using a Bell state as the initial coin state, two different coin operators, two different shift operators, and one walker. We compare and contrast the performance of these quantum walks with that of a classical random walk consisting of one walker and two maximally correlated coins as well as quantum walks with coins sharing different degrees of entanglement.

We illustrate that the behaviour of our walk with entangled coins can be very different in comparison to the usual quantum walk with a single coin. We also demonstrate that simply by changing the shift operator, we can generate widely different distributions. We also compare the behaviour of quantum walks with maximally entangled coins with that of quantum walks with non-entangled coins. Finally, we show that the use of different shift operators on 2 and 3 qubit coins leads to different position probability distributions in 1 and 2 dimensional graphs.

PACS numbers:

I. INTRODUCTION

In recent years interest in the field of Quantum Walks has grown hugely, motivated by the importance of Classical Random Walks in Computer Science, as well as the advantages that Quantum Walks may provide us with when compared to their classical counterparts.

Classical random walks are a fundamental tool in Computer Science due to their use in the development of stochastic algorithms [1]. In both theoretical and applied Computer Science, stochastic algorithms may outperform any deterministic algorithm built to solve certain problems. A notable example is that of the best algorithm known so far for the solution of 3-SAT, a fundamental problem in Computer Science which relies on random walks techniques [2].

So random walks are important elements of Computer Science. Additionally, the recent development of Quantum Computation and Quantum Information has revealed that the exploitation of inherently quantum mechanical systems for computational purposes leads to a number of significant advantages over purely classical systems. Thus it is reasonable to expect that the study of random walks using quantum mechanical systems may prove fruitful. The basic properties of two kinds of quantum walks have already received a good deal of attention: continuous ([3] - [9]) and discrete ([10] - [16]) quantum walks. In this paper we shall focus on discrete quantum walks.

Quantum walks are expected to play a major role in the field of Quantum Algorithms. A number of benefits of employing such walks are already known. In [20], Childs *et al* have built a quantum algorithm based on a continuous quantum walk to solve the problem of traversing a graph G with an exponential number of vertices under a vertex connectivity arrangement. It was proved in [20] that traversing such a graph with their

quantum algorithm is exponentially faster than doing so with any classical algorithm. Additionally, it has been proved by Ambainis *et al* that quantum walks on a line spread quadratically faster than classical random walks [17], while Kempe [18] proved that the hitting time of a quantum walk on the hypercube is polynomial in the number of steps of the walk (the classical counterpart takes exponential time). Also, Shenvi *et al* [19] showed that quantum walks can be used to produce a quantum search algorithm. Finally, an algorithm based on quantum walks to solve the problem of element distinctness can be found in [21]. An excellent summary of the basics of quantum walks can be found in [22], and a compendium of algorithmic applications of quantum walks is presented in [23].

A discrete quantum walk is composed of two physical systems: a walker and a coin (a detailed explanation of these two systems is provided in Section III). The properties of quantum walks applying multiple quantum coin operators ([24] - [26]) as well as decoherent coins ([27] - [29]) on a single walker have been extensively studied.

However, the use of entanglement in quantum walks is less well explored. A discussion on discrete quantum walks using non-separable evolution operators and its effects on the standard deviation of resulting probability distributions is given in [35], followed by [25] where a more exhaustive study on non-separable operators is provided. In [30], Du *et al* proposed an implementation of a continuous quantum walk on a circle, and numerically showed that entanglement in the position states shapes the position probability distribution. More recently, a discussion concerning models of a quantum walk on a line with two entangled particles as walkers is provided in [34]. A study of entanglement between coin and walker in quantum walks on graphs is given in [31], along with a generalization of the quantum walk algorithm from [20]. In [32] the authors analyse the relation between

coin entanglement and the mean position of the quantum walker for 3 and 4 qubit coins. Finally, in [33], Abal *et al* have quantified the entanglement between walker and coin generated by the shift operator in a single coin-single walker quantum walk.

Our motivation to use entangled coins in quantum walks comes from two sources. First, using entangled coins $|c\rangle \in \mathcal{H}^n$ in quantum walks on graphs $G(V, E)$ with $\deg(v_i) = m \forall v_i \in V$ in which $n > m$, motivates the employment of different shift operators and therefore expands the dynamics of the quantum walk. In particular, in this paper we use maximally entangled coins in quantum walks on an infinite line along with shift operators with “rest sites”, i.e. states that allow the walker to stay at the current vertex. Indeed, it is also possible to introduce pairs of coins in a classical random walk on an infinite line in order to expand its dynamics, but that is at the expense of varying the amount of correlation between the random variables produced with the outcomes of corresponding coins.

Second, an entangled coin comprised of two qubits, each residing in \mathcal{H}^2 , can be viewed as a single coin defined on \mathcal{H}^4 , and then appropriately partitioned. Indeed the orthonormal basis $\{|00\rangle, |01\rangle, |10\rangle, |11\rangle\}$ spans the space \mathcal{H}^4 . However, the phenomenon of entanglement represents a supercorrelation between possibly spacelike-separated subsystems of a total quantum system. It is certainly feasible to generate entanglement between two qubits and then separate them either for the purposes of an experiment in the laboratory, for example to allow for individual addressing of each qubit in some quantum information processing experiment (such as implementing the Hadamard operator), or to send them to opposite sides of the universe. This pre-existing entanglement resource is created during a finite time period of interaction and then the distinct subsystems can be separated to arbitrary locations. However, a single four-level quantum system cannot be physically broken and spatially separated into two pieces so that each piece is subsequently subjected to local operations. Partitioning a single coin into two entangled subsystems is nevertheless equivalent to using two distinct entangled coins, provided that the subsystems do not require to be physically separated for practical purposes. Although the mathematical description is the same, we choose to work with a pair of entangled qubits. Generation of photonic entangled states, for example by way of spontaneous parametric downconversion, or entangled states in ion traps, is already experimentally achievable. As such, identifying the entangled coins as bipartite states, rather than single an appropriately partitioned single system residing in \mathcal{H}^4 , is a natural choice to highlight and motivate possible links to experiment.

Two specific physical implementations of quantum walks, namely cavity-QED based [42] and ion-trap based [43] motivate the scenario considered by us. In both these implementations, two-level atoms serve as coins, while a cavity mode [42] or a vibrational mode [43] serve

as the walker. Two atomic qubits in an ion trap are already feasible, and have been prepared in Bell states [44] and there are several proposals for entangling two atomic qubits in a cavity, such as [45]. These atoms can then be used as entangled coins with a common cavity mode or the common ion trap vibrational mode acting as the walker controlled by both these coins. While it is straightforward to treat the two atoms as individual qubits during this process, it is rather difficult to do entangling operations between them during the walk without using/affecting the cavity or vibrational mode which is already acting as the walker. Of course, a cavity mode or vibrational mode other than the one acting as walker may be used to do entangling gates between the atoms, but this is complicated. Moreover, in some cases, no method of accomplishing a direct unitary entangling gate between two atoms may be present, and their initial entanglement (needed for the walk considered here) may have been produced using other mechanisms (such as decays and measurements [45]). Because of this inherent difficulty of doing an entangling gate between the coins during a quantum walk, it is easier to imagine a scenario of two entangled coin qubits rather than a single four dimensional coin. Once two atoms have been trapped and entangled in a cavity, and this has already been done for ion traps, the implementation of our scenario is no more complex than a single coin quantum walk as the same global fields can be applied to both atoms for the coin and the shift operations (there is no need for addressing the atoms separately).

In this paper we shall discuss the behaviour of a quantum walk on an infinite line (also called unrestricted quantum walk) with one coin composed of two maximally entangled particles, and one walker. We compare the performance of such a walk with that of a classical random walk with one walker and two maximally correlated coins. We also show that the use of different shift operators on 2 and 3 qubit coins leads to different position probability distributions in both one and two-dimensional graphs.

The idea behind correlated coins is simple. For a pair of correlated coins C_1 and C_2 with corresponding outcomes (H_1, T_1) and (H_2, T_2) one expects that, after obtaining a certain outcome for coin C_1 , coin C_2 will produce its corresponding outcome *according to a probability distribution defined by the degree of correlation between both coins*.

For example, the behaviour of a maximally correlated pair of coins would be the following: outcomes for coin C_1 would be given according to a certain probability distribution. Let us suppose that coin C_1 is unbiased, thus outcomes H_1 and T_1 may each occur with equal probability. Now let us suppose that we get H_1 (T_1) as outcome. Since the coin pair is maximally correlated, then the outcome for coin C_2 will certainly be H_2 (T_2).

If the degree of correlation were less than maximal between coins C_1 and C_2 , then obtaining outcome H_1 for C_1 would imply that the probability of getting H_2 as outcome for coin C_2 would not be unity. In fact the proba-

bility would scale as a monotonically increasing function of the degree of correlation between the coins.

Using correlated coins in classical random walks is straightforward. For a classical random walk with a maximally correlated pair of coins it is natural to assign the walker one step to the right whenever the pair (H_1, H_2) (say) is the resulting outcome, and one step to the left for the outcome (T_1, T_2) (say). In this case, outcomes (H_1, T_2) and (T_1, H_2) have probability zero.

Indeed, we could enrich our classical random walk by allowing coin outcomes $O_3 = (H_1, T_2)$ and $O_4 = (T_1, H_2)$. For example, one could use outcome O_3 to permit the walker to remain in its current position or, alternatively, all four outcomes could be used to perform a random walk with 1 and 2 steps to the right and left, respectively. In particular, the introduction of outcomes that allow rest states is a feature used to remove the parity property of classical random walks, which consists of finding the walker only in even (odd) positions in an even (odd) time step. However, the introduction of outcomes O_3 and O_4 implies that the coin pair would no longer be maximally correlated.

In the following section we formally introduce a classical random walk with a maximally correlated pair of coins. In Section III we present a brief background introduction to unrestricted quantum walks on a line with a single coin, followed by our results on unrestricted quantum walks on a line with a maximally entangled coin.

Our results show that probability distributions of quantum walks with maximally entangled coins have particular shapes that are highly invariant to changes in coin operators. These results are then compared with those obtained for classical random walks with maximally correlated coins.

II. CLASSICAL RANDOM WALK WITH 2 MAXIMALLY CORRELATED COINS

A classical result from stochastic processes states that, for an unrestricted classical random walk starting at position $z_0 = 0$, the probability of finding the walker at position k after n steps, when with probability p the walker takes a step to the right and with probability $q = 1 - p$ takes a step to the left (i.e. tossing the coin with probability p of obtaining outcome T and probability q of obtaining outcome H), is given by

$$P_{ok}^{(n)} = \binom{n}{\frac{1}{2}(k+n)} p^{\frac{1}{2}(k+n)} q^{\frac{1}{2}(n-k)} \quad (1)$$

for $\frac{1}{2}(k+n) \in \{0, 1, \dots, n\}$ and 0 otherwise.

Tossing a pair of coins produces two discrete random variables C_1 and C_2 , and the correlation ρ between these two random variables is given by ([36])

$$\rho(C_1, C_2) = \frac{\text{Cov}(C_1, C_2)}{\sqrt{\text{Var}(C_1)\text{Var}(C_2)}} \quad (2)$$

where $\text{Cov}(X, Y)$ and $\text{Var}(X)$ are the covariance and the variance of the corresponding random variables. The function ρ is bounded by $-1 \leq \rho \leq 1$. $\rho(C_1, C_2) = 0$ means that random variables C_1 and C_2 are totally uncorrelated (i.e. C_1 and C_2 are independent), whereas $\rho(C_1, C_2) = 1$ means that random variables C_1 and C_2 are maximally correlated. The case $\rho(C_1, C_2) = -1$ corresponds to perfect anticorrelation.

Now consider a classical random walk that has a maximally correlated pair of coins, i.e. $\rho(C_1, C_2) = 1$. Also suppose that the first coin C_1 is unbiased. Then, as explained in the previous section, the only two outcomes allowed for this coin pair are $O_1 = (H_1, H_2)$ or $O_2 = (T_1, T_2)$. If O_1 allows the walker to move one step to the left and O_2 allows the walker to move one step to the right, it is then clear that using such a coin pair in a classical random walk would produce a probability distribution equal to that of Eq. (1), with $p = \frac{1}{2}$. A plot of Eq. (1) with number of steps $n = 100$ and $p = \frac{1}{2}$ is provided in Fig. (1) for the purpose of comparison with results presented in Section III.

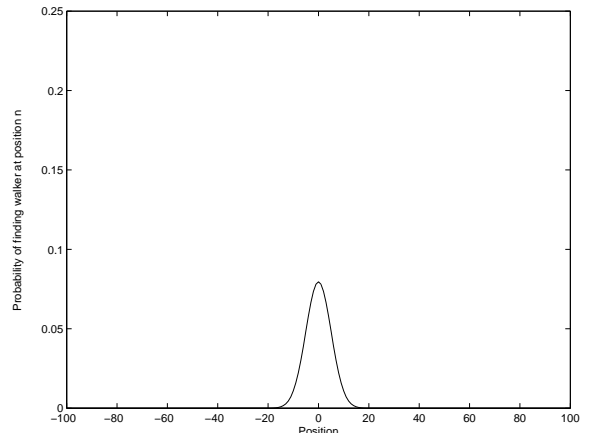


FIG. 1: Plot of $P_{ok}^{(n)} = \binom{n}{\frac{1}{2}(k+n)} p^{\frac{1}{2}(k+n)} q^{\frac{1}{2}(n-k)}$ for $n = 100$ and $p = \frac{1}{2}$. The probability of finding the walker in position $k = 0$ is equal to 0.0795. Only probabilities corresponding to even positions are shown, as odd positions have probability equal to zero.

As can be seen in Fig.(1), the use of maximally correlated unbiased coins in classical random walks is not different with respect to a classical random walk with a single unbiased coin, as the probability distributions from both kinds of classical random walks are exactly the same.

In the following sections we shall compare the results obtained by the computation of classical random walks with maximally correlated (classical) coins with those of quantum walks with maximally entangled (quantum correlated) coins.

III. QUANTUM WALKS WITH ENTANGLED COINS

A. Review of Quantum Walks on an Infinite Line

We now review the mathematical structure of a quantum walk on a line with one coin and a single walker, with a view to using this structure to construct a model for unrestricted quantum walks on the line with a maximally entangled coin.

The main components of a quantum walk on a line are a walker, a coin, evolution operators for both walker and coin, and a set of observables:

Walker and Coin: The walker is a quantum system living in a Hilbert space of infinite but countable dimension \mathcal{H}_p . It is customary to use vectors from the canonical (computational) basis of \mathcal{H}_p as “position sites” for the walker. So, we denote the walker as $|\text{position}\rangle \in \mathcal{H}_p$ and affirm that the canonical basis states $|i\rangle_p$ that span \mathcal{H}_p , as well as any superposition of the form $\sum_i \alpha_i |i\rangle_p$ subject to $\sum_i |\alpha_i|^2 = 1$, are valid states for $|\text{position}\rangle$. The walker is usually initialized at the ‘origin’, i.e. $|\text{position}\rangle_{\text{initial}} = |0\rangle_p$.

The coin is a quantum system living in a 2-dimensional Hilbert space \mathcal{H}_c . The coin may take the canonical basis states $|0\rangle$ and $|1\rangle$ as well as any superposition of these basis states. Therefore $|\text{coin}\rangle \in \mathcal{H}_c$ and a general normalized state of the coin may be written as $|\text{coin}\rangle = a|0\rangle_c + b|1\rangle_c$, where $|a|^2 + |b|^2 = 1$.

The total state of the quantum walk resides in $\mathcal{H}_t = \mathcal{H}_p \otimes \mathcal{H}_c$. Only product states of \mathcal{H}_t have been used as initial states, that is, $|\psi\rangle_{\text{initial}} = |\text{position}\rangle_{\text{initial}} \otimes |\text{coin}\rangle_{\text{initial}}$.

Evolution Operators: The evolution of a quantum walk is divided into two parts that closely resemble the behaviour of a classical random walk. In the classical case, chance plays a key role in the evolution of the system. This is evident in the following example: we first toss a coin (either biased or unbiased) and then, depending on the coin outcome, the walker moves one step either to the right or to the left.

In the quantum case, the equivalent of the previous process is to apply an evolution operator to the coin state followed by a conditional shift operator to the total system. The purpose of the coin operator is to render the coin state in a superposition, and the randomness is introduced by performing a measurement on the system after both evolution operators have been applied to the total quantum system several times.

Among coin operators, customarily denoted by \hat{C} , the Hadamard operator

$$\hat{H} = \frac{1}{\sqrt{2}}(|0\rangle_{cc}\langle 0| + |0\rangle_{cc}\langle 1| + |1\rangle_{cc}\langle 0| - |1\rangle_{cc}\langle 1|) \quad (3)$$

has been extensively used.

For the conditional shift operator use is made of a unitary operator that allows the walker to go one step forward if the accompanying coin state is one of the two

basis states (e.g. $|0\rangle$), or one step backwards if the accompanying coin state is the other basis state ($|1\rangle$). A suitable conditional shift operator has the form

$$\begin{aligned} \hat{S} = & |0\rangle_{cc}\langle 0| \otimes \sum_i |i+1\rangle_{pp}\langle i| \\ & + |1\rangle_{cc}\langle 1| \otimes \sum_i |i-1\rangle_{pp}\langle i|. \end{aligned} \quad (4)$$

Consequently, the operator on the total Hilbert space is $\hat{U} = \hat{S} \cdot (\hat{C} \otimes \hat{\mathbb{I}}_p)$ and a succinct mathematical representation of a quantum walk after n steps is $|\psi\rangle = (\hat{U})^n |\psi\rangle_{\text{initial}}$, where $|\psi\rangle_{\text{initial}} = |\text{position}\rangle_{\text{initial}} \otimes |\text{coin}\rangle_{\text{initial}}$.

Observables: The advantages of quantum walks over classical random walks are a consequence of interference effects between coin and walker after several applications of \hat{U} . However, we must perform a measurement at some point in order to know the outcome of our walk. To do so, we define a set of observables according to the basis states that have been used to define coin and walker.

In order to extract information from the composite quantum system, we first perform a measurement on the coin using the observable

$$\hat{M}_c = \alpha_0 |0\rangle_{cc}\langle 0| + \alpha_1 |1\rangle_{cc}\langle 1|. \quad (5)$$

A measurement must then be performed on the position states of the walker by using the operator

$$\hat{M}_p = \sum_i a_i |i\rangle_{pp}\langle i|. \quad (6)$$

B. Mathematical Structure of Quantum Walks on an Infinite Line Using a Maximally Entangled Coin

As before, the elements of an unrestricted quantum walk on a line are a walker, a coin, evolution operators for both coin and walker, and a set of observables. We shall provide a detailed description of each element motivated by the previous subsection.

Walker and Coin: The walker is, as in the unrestricted quantum walk with a single coin, a quantum system $|\text{position}\rangle$ residing in a Hilbert space of infinite but countable dimension \mathcal{H}_P . The canonical basis states $|i\rangle_P$ that span \mathcal{H}_P , as well as any superposition of the form $\sum_i \alpha_i |i\rangle_p$ subject to $\sum_i |\alpha_i|^2 = 1$, are valid states for the walker. The walker is usually initialized at the ‘origin’ i.e. $|\text{position}\rangle_0 = |0\rangle_P$.

The coin is now an entangled system of two qubits i.e. a quantum system living in a 4-dimensional Hilbert space \mathcal{H}_{EC} . We denote coin initial states as $|\text{coin}\rangle_0$. Also, we shall use the following Bell states as coin initial states

$$|\Phi^+\rangle = \frac{1}{\sqrt{2}}(|00\rangle + |11\rangle) \quad (7a)$$

$$|\Phi^-\rangle = \frac{1}{\sqrt{2}}(|00\rangle - |11\rangle) \quad (7b)$$

$$|\Psi^+\rangle = \frac{1}{\sqrt{2}}(|01\rangle + |10\rangle) \quad (7c)$$

which are maximally entangled pure bipartite states with reduced von Neumann entropy equal to unity. We shall examine the consequences of employing such maximally entangled states by comparing the resulting walks with those resulting from using maximally correlated coins in classical random walks. The Bell singlet state $|\Psi^-\rangle = \frac{1}{\sqrt{2}}(|01\rangle - |10\rangle)$ is not employed as an entangled coin as it is left invariant when the same local unitary operator is applied to both coins.

The total initial state of the quantum walk resides in the Hilbert space $\mathcal{H}_T = \mathcal{H}_P \otimes \mathcal{H}_{EC}$ and has the form

$$|\psi\rangle_0 = |\text{position}\rangle_0 \otimes |\text{coin}\rangle_0 \quad (8)$$

Entanglement measure: In order to quantify the degree of entanglement of the coins used in this paper, we shall employ the reduced von Neumann entropy measure. For a pure quantum state $|\psi\rangle$ of a composite system AB with $\dim(A) = d_A$ and $\dim(B) = d_B$, let $|\psi\rangle = \sum_{i=1}^d \alpha_i |i_A\rangle |i_B\rangle$, ($d = \min(d_A, d_B)$, $\alpha_i \geq 0$ and $\sum_{i=1}^d \alpha_i^2 = 1$) be its Schmidt decomposition. Also, let $\rho_A = \text{tr}_B(|\psi\rangle\langle\psi|)$ and $\rho_B = \text{tr}_A(|\psi\rangle\langle\psi|)$ be the reduced density operators of systems A and B respectively. The entropy of entanglement $E(|\psi\rangle)$ is the von Neumann entropy of the reduced density operator [37]

$$E(|\psi\rangle) = S(\rho_A) = S(\rho_B) = - \sum_{i=1}^d \alpha_i^2 \log_2(\alpha_i^2). \quad (9)$$

E is a monotonically-increasing function of the entanglement present in the system AB . A non-entangled state has $E = 0$. States $|\psi\rangle \in \mathcal{H}^d$ for which $E(\psi) = d$ are called *maximally entangled states* in d dimensions. In particular, note that for those quantum states described by Eqs. (7a), (7b) and (7c) $E(|\Phi^+\rangle) = E(|\Phi^-\rangle) = E(|\Psi^+\rangle) = 1$, i.e. these states are maximally entangled.

Evolution Operators: The evolution operators used are more complex than those for quantum walks with single coins. As in the single coin case, the only requirement evolution operators must fulfil is that of unitarity.

Let us start by defining evolution operators for an entangled coin. Since the coin is a bipartite system, its evolution operator is defined as the tensor product of two single-qubit coin operators:

$$\hat{C}_{EC} = \hat{C} \otimes \hat{C} \quad (10)$$

For example, we could define the operator \hat{C}_{EC}^H as the tensor product $\hat{H}^{\otimes 2}$:

$$\begin{aligned} \hat{C}_{EC}^H = & \frac{1}{2}(|00\rangle\langle 00| + |01\rangle\langle 00| + |10\rangle\langle 00| + |11\rangle\langle 00| \\ & + |00\rangle\langle 01| - |01\rangle\langle 01| + |10\rangle\langle 01| - |11\rangle\langle 01| \\ & + |00\rangle\langle 10| + |01\rangle\langle 10| - |10\rangle\langle 10| - |11\rangle\langle 10| \\ & + |00\rangle\langle 11| - |01\rangle\langle 11| - |10\rangle\langle 11| + |11\rangle\langle 11|). \end{aligned} \quad (11)$$

An alternative bipartite coin operator is produced by computing the tensor product $\hat{Y}^{\otimes 2}$ where $\hat{Y} = \frac{1}{\sqrt{2}}(|0\rangle\langle 0| + i|0\rangle\langle 1| + i|1\rangle\langle 0| + |1\rangle\langle 1|)$, namely

$$\begin{aligned} \hat{C}_{EC}^Y = & \frac{1}{2}(|00\rangle\langle 00| + i|01\rangle\langle 00| + i|10\rangle\langle 00| - |11\rangle\langle 00| \\ & + i|00\rangle\langle 01| + |01\rangle\langle 01| - |10\rangle\langle 01| + i|11\rangle\langle 01| \\ & + i|00\rangle\langle 10| - |01\rangle\langle 10| + |10\rangle\langle 10| + i|11\rangle\langle 10| \\ & - |00\rangle\langle 11| + i|01\rangle\langle 11| + i|10\rangle\langle 11| + |11\rangle\langle 11|). \end{aligned} \quad (12)$$

Both coin operators are fully separable, thus any entanglement in the coins is due to the initial states used.

The conditional shift operator \hat{S}_{EC} necessarily allows the walker to move either forwards or backwards along the line, depending on the state of the coin. The operator

$$\begin{aligned} \hat{S}_{EC} = & |00\rangle_{cc}\langle 00| \otimes \sum_i |i+1\rangle_{pp}\langle i| \\ & + |01\rangle_{cc}\langle 01| \otimes \sum_i |i\rangle_{pp}\langle i| \\ & + |10\rangle_{cc}\langle 10| \otimes \sum_i |i\rangle_{pp}\langle i| \\ & + |11\rangle_{cc}\langle 11| \otimes \sum_i |i-1\rangle_{pp}\langle i| \end{aligned} \quad (13)$$

embodies the stochastic behaviour of a classical random walk with a maximally correlated coin pair. It is only when both coins reside in the $|00\rangle$ or $|11\rangle$ state that the walker moves either forwards or backwards along the line; otherwise the walker does not move.

Note that \hat{S}_{EC} is one of a family of valid definable shift operators. Indeed, it might be troublesome to identify a classical counterpart for some of these operators: their existence is uniquely quantum-mechanical in origin. One such alternative operator is

$$\begin{aligned} \hat{S}'_{EC} = & |00\rangle_{cc}\langle 00| \otimes \sum_i |i+2\rangle_{pp}\langle i| \\ & + |01\rangle_{cc}\langle 01| \otimes \sum_i |i+1\rangle_{pp}\langle i| \\ & + |10\rangle_{cc}\langle 10| \otimes \sum_i |i-1\rangle_{pp}\langle i| \\ & + |11\rangle_{cc}\langle 11| \otimes \sum_i |i-2\rangle_{pp}\langle i|. \end{aligned} \quad (14)$$

The total evolution operator has the structure $\hat{U}_T = \hat{S}_{EC} \cdot (\hat{C}_{EC} \otimes \hat{\mathbb{I}}_p)$ and a succinct mathematical representation of a quantum walk after N steps is $|\psi\rangle = (\hat{U}_T)^N |\psi\rangle_0$, where $|\psi\rangle_0$ denotes the initial state of the walker and the coin.

Observables: The observables defined here are used to extract information about the state of the quantum walk $|\psi\rangle = (\hat{U}_T)^N |\psi\rangle_0$.

We first perform measurements on the coin using the observable

$$\hat{M}_{EC} = \beta_{00}|00\rangle_{cc}\langle 00| + \beta_{01}|01\rangle_{cc}\langle 01| + \beta_{10}|10\rangle_{cc}\langle 10| + \beta_{11}|11\rangle_{cc}\langle 11|. \quad (15)$$

Measurements are then performed on the position states using the operator

$$\hat{M}_P = \sum_j b_j |j\rangle_{PP}\langle j|. \quad (16)$$

With the purpose of introducing the results presented in the rest of this paper we compare in Table 1 the actual position probability values for a classical random walk on an infinite line (Eq. (1)), and a quantum walk with initial state $|\Phi^+\rangle = \frac{1}{\sqrt{2}}(|00\rangle + |11\rangle)$ and coin and shift operators given by Eqs. (11) and (13), respectively.

Table 1. Position Probability values for classical random walk and quantum walk

Classical	-3	-2	-1	0	1	2	3
Step 0	0	0	0	1	0	0	0
Step 1	0	0	1/2	0	1/2	0	0
Step 2	0	2/8	0	4/8	0	2/8	0
Step 3	4/32	0	12/32	0	12/32	0	4/32

Quantum	-3	-2	-1	0	1	2	3
Step 0	0	0	0	1	0	0	0
Step 1	0	0	1/2	0	1/2	0	0
Step 2	0	1/8	2/8	2/8	2/8	1/8	0
Step 3	1/32	6/32	5/32	8/32	5/32	6/32	1/32

C. Results for Quantum Walks on an Infinite Line Using a Maximally Entangled Coin

In order to investigate the properties of unrestricted quantum walks with entangled coins, we have computed several simulations using bipartite maximally entangled coin states described by Eqs. (7a), (7b) and (7c), and coin evolution operators described by Eqs. (11) and (12). In all cases, the initial position state of the walker corresponds to the origin, i.e. $|\text{position}\rangle_0 = |0\rangle$. The shift operator employed is, with the exception of Fig. (8), that of Eq. (13).

Let us first discuss the quantum walks whose graphs are shown in Fig. (2). The initial entangled coin state is given by Eq. (7a) and the number of steps is 100. For the red plot in Fig. (2) the coin operator is given by Eq. (11), while for the dotted blue plot in the same Fig. (2) the coin operator is that of Eq. (12).

The first notable property of these quantum walks is that, unlike the classical case in which the most probable location of the walker is at the origin and the probability

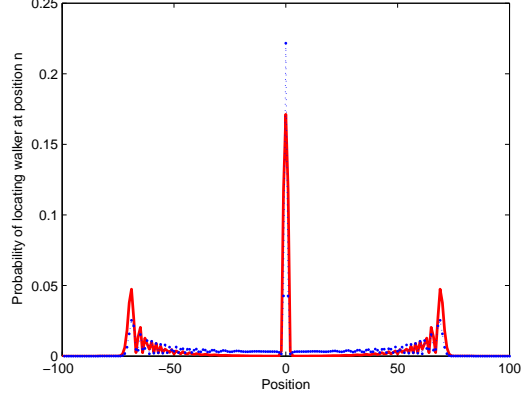


FIG. 2: For both plots, coin initial state is $|\Phi^+\rangle = \frac{1}{\sqrt{2}}(|00\rangle + |11\rangle)$ and the number of steps is 100. Coin operators for red and dotted blue plots are given by Eq. (11) and Eq. (12) respectively.

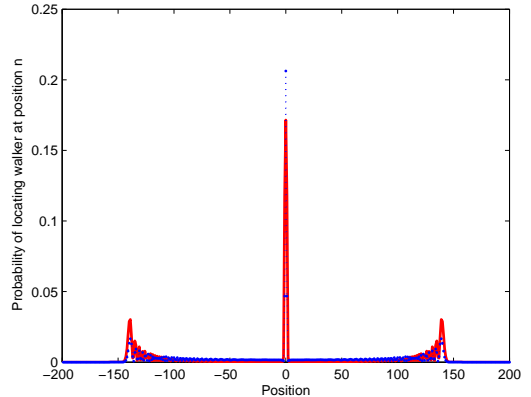


FIG. 3: For both plots, coin initial state is $|\Phi^+\rangle = \frac{1}{\sqrt{2}}(|00\rangle + |11\rangle)$ and the number of steps is 200. Coin operators for red and dotted blue plots are given by Eq. (11) and Eq. (12) respectively.

distribution has a single peak, in the quantum case a certain range of very likely positions about the position $|0\rangle$ is evident but in addition there are a further two regions at the extreme zones of the walk in which it is likely to find the particle. This is the ‘three peak zones’ property of the shift operator defined in this way. The ‘three peak zones’ property could mean an additional advantage of quantum walks over classical random walks.

We also note that the probability of finding the walker in the most likely position, $|0\rangle$, is much higher in the quantum case (~ 0.171242 in red plot of Fig. (2) and ~ 0.221622 in dotted blue plot of Fig. (2)) than in the classical case (~ 0.0795). Incidentally, we find that the use of different coin initial states maintains the basic structure of the probability distribution, unlike the quantum walk with a single coin in which the use of different coin initial states can lead to different probability distri-

butions ([13], [39] and [40]) .

The position probability distributions shown in Fig. (2) could embody some advantages when used in an appropriate application framework. For example, let us suppose we want to design algorithms whose purpose is to find the wrong values in a proposed solution of a problem (a concrete case is to find all wrong binary values assigned to the initial conditions of the algorithm used in [38] to find a solution to the 3-SAT problem.) We use a 100-steps classical random walk (Fig. (1)) to design algorithm C and a 100-steps quantum walk with maximally entangled coins (red plot of Fig. (2)) to design algorithm Q .

Depending on the actual number of wrong values, the probability distribution of red plot of Fig. (2) could help to make algorithm Q faster than algorithm C . For example, if the number of wrong values is in the range 40 - 70, the probability of finding the quantum walker of Fig. (2) is much higher than finding the classical walker of Fig. (1). Actual probability values (note the differences in orders of magnitude) are shown in Table 2. It must be noted that employing a quantum walk on a line with a single coin for building algorithm Q would also produce higher probability values than a classical random walk in those positions shown in Table 2, thus the choice of quantum walk could depend on some other factors like implementation feasibility.

Table 2. Position Probabilities for Classical and Quantum Walkers

Position	Classical Walker	Quantum Walker
40	2.31×10^{-5}	1.80×10^{-3}
50	1.91×10^{-7}	1.50×10^{-3}
60	4.22×10^{-10}	1.03×10^{-2}
70	1.99×10^{-13}	3.78×10^{-2}

A consequence of the previous two properties of the quantum walk is a sharper and narrower peak in the probability distribution around position $|0\rangle$. Again, this may be of some advantage depending on the application of the quantum walk (for example, less dispersion around the most likely solution to the computational problem posed in the two previous paragraphs).

The probability distributions for quantum walks in Fig. (3) are very similar in structure to those of Fig. (2), the only difference being the number of steps (200 as opposed to 100). For Fig. (3) the initial entangled coin state is given by Eq. (7a). Eq. (11) is used as the coin operator in the red plot of Fig. (3) whereas Eq. (12) is the coin operator for the dotted blue plot of Fig. (3). For 200 steps the peaks on both extreme zones are smaller than for 100 steps, the reason being the increased number of small probabilities that correspond to those regions between the extreme peaks and the central peak. A wider region is covered in the case of 200 steps than for 100 steps.

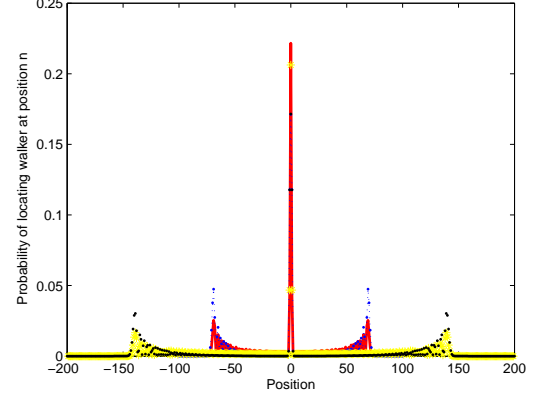


FIG. 4: Coin initial state is $|\Phi^-\rangle = \frac{1}{\sqrt{2}}(|00\rangle - |11\rangle)$. Number of steps is 100 for red and dotted blue plots and 200 for starred yellow and black dotted plots. Coin operator for red and starred yellow plots is given by Eq. (11), while coin operators for dotted blue and dotted black plots is given by Eq. (12) respectively.

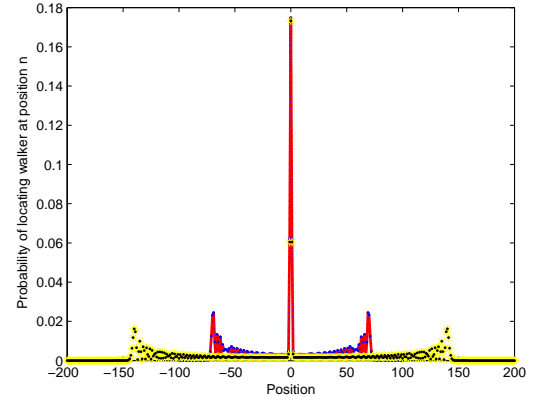


FIG. 5: Coin initial state is $|\Psi^+\rangle = \frac{1}{\sqrt{2}}(|01\rangle + |10\rangle)$. Number of steps is 100 for red and dotted blue plots and 200 for starred yellow and black dotted plots. Coin operator for red and starred yellow plots is given by Eq. (11), while coin operators for dotted blue and dotted black plots is given by Eq. (12) respectively.

An examination of Figs. (4) and (5) is straightforward, as their bulk properties closely resembling those of Fig. (2) and Fig. (3). The probability distributions in Fig. (4) and Fig. (5) were computed using Eq. (7b) as the initial coin state and the same initial conditions and shift operators as for Fig. (2) and Fig. (3). The number of steps is 100 for red and dotted blue plots and 200 for starred yellow and black dotted plots. Coin operator for red and starred yellow plots is given by Eq. (11), while coin operators for dotted blue and dotted black plots is given by Eq. (12) respectively. The ‘three-peak zones’ feature is again evident. Furthermore, the bulk properties of the probability distributions are highly invariant to changes

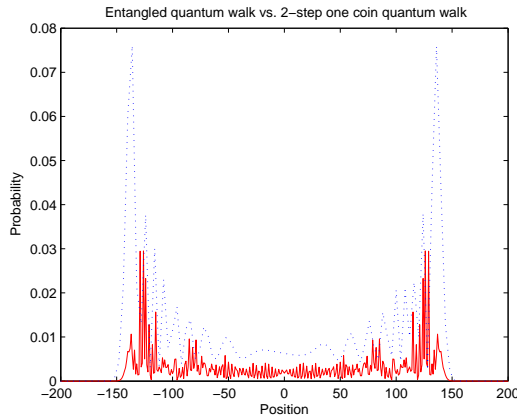


FIG. 6: For the red line plot, the coin initial state is given by $|\Psi^+\rangle = \frac{1}{\sqrt{2}}(|00\rangle + |11\rangle)$. Coin operator is given by Eq. (11) and shift operator by Eq. (14). For the blue dashed graph, coin initial state is given by $(\sqrt{0.85}|0\rangle_c - \sqrt{0.15}|1\rangle_c)$, coin operator is the Hadamard operator (Eq. (3)) as coin operator and shift operator given by $|0\rangle\langle 0| \otimes \sum_i |i+2\rangle\langle i| + |1\rangle\langle 1| \otimes \sum_i |i-2\rangle\langle i|$. In both cases, the number of steps is 100.

in coin operators (there is a slight difference in the probability distribution value at the origin). In both cases the probability distribution value at the origin is much larger than in the classical random walk case. A similar discussion having Eq. (7c) as coin initial state, and using the same colors as in Fig. (4) to refer to coin operators and number of steps, applies to Fig. (5).

In order to further motivate the richness of quantum walks with entangled coins, we present the graph shown in Fig. (6, red line plot) computed using Eq. (7a) as the initial state of the coin, Eq. (11) as the coin operator and Eq. (14) as the shift operator. This graph closely resembles that of a 2-step quantum walk Fig. (6, dotted blue plot) with initial state $(\sqrt{0.85}|0\rangle_c - \sqrt{0.15}|1\rangle_c) \otimes |0\rangle_p$ [25], Hadamard operator (Eq. (3)) as coin operator and shift operator given by $|0\rangle\langle 0| \otimes \sum_i |i+2\rangle\langle i| + |1\rangle\langle 1| \otimes \sum_i |i-2\rangle\langle i|$ (the number of steps in both walks is 100). However, the graph corresponding to the quantum walks with a maximally entangled coin has no parity restriction, as opposed to the 2-step quantum walk, and this explains the higher probability values for the 2-step quantum walks.

As opposed to the previous cases (Figs. 2 - 5) in which the walker remains static when the quantum coin state component is either $|01\rangle$ or $|10\rangle$, in this case the walker is forced to jump either one or two steps, depending on the components of the coin state. As can be seen in Fig. (6), the behaviour of the quantum walk dramatically changes as a consequence of the change in the shift operator. In this case, constructive interference takes place not only in certain areas of the graph (as is the case with the ‘three peak zones’ property) but in a wider region. Indeed, this walk bears a resemblance to a quantum walk using a single walker and a single Hadamard coin [22].

Finally we would like to emphasize that in stark con-

trast to the probability distributions of the classical case in which only certain walker positions have a probability different from zero, namely those positions whose parity is that of the total number of steps, in the quantum cases presented in this paper we observe no such constraint on the numerical data produced. As stated in the introduction, the dynamics of classical random walks can remove the parity constraint by permitting the use of ‘rest sites’ at the expense of varying the amount of correlation between the coins.

IV. QUANTUM WALKS USING COINS WITH DIFFERENT VALUES OF ENTANGLEMENT

In order to compare the properties of quantum walks with coins having different degrees of entanglement, we present in this section several probability distributions computed using bipartite coins. The graphs of those probability distributions are shown in Figs. (7 - 9). All graphs shown in Figs. (7 - 9) were computed using Eq. (11) as coin operator and Eq. (13) as shift operator. The initial position state in all cases is the origin, i.e. $|0\rangle_p$.

The probability distribution presented in Fig. (7) shows a typical skewed (asymmetric) behaviour in quantum walks. The graph is produced using the bipartite quantum state $|\theta_0\rangle = \frac{1}{2}(|0\rangle + |1\rangle)(|0\rangle + |1\rangle)$ as coin initial state (from Eq. (9), $E(|\theta_0\rangle) = 0$ so $|\theta_0\rangle$ is non-entangled). This graph resembles the behaviour of a quantum walk presented in [29] using a coin in initial state $|00\rangle$ ($|RR\rangle$ in their notation).

Let us now focus on the behaviour of the quantum walk shown in Fig. (8), which was produced using a partially entangled initial coin state. The coin was initialized in the state $|\theta_1\rangle = \frac{1}{2}|00\rangle + \frac{1}{2}|01\rangle + \frac{\sqrt{3}-1}{4}|10\rangle + \frac{\sqrt{3}+1}{4}|11\rangle$. Again, using Eq. (9), we find that $E(|\theta_1\rangle) = 0.5$, i.e. $|\theta_1\rangle$ is partially entangled.

We can see that an immediate effect of an entangled coin initial state is the development of a third peak, in the case a peak on the LHS of the graph. This third peak reduces the skewness of the probability distribution computed with a non-entangled coin initial state (Fig. (9)).

Let us now compare Figs. (9) and (10) with the red plot from Fig. (2), created with the maximally entangled state $\frac{1}{\sqrt{2}}(|00\rangle + |11\rangle)$ as initial coin state. We can see that the increasing use of entanglement provides a greater degree of symmetry to the resulting probability distribution.

Now, if we expand the properties of initial conditions by allowing coins to be initialized in states with complex coefficients, we would then obtain probability distributions that would be similar to those of quantum walks with maximally entangled coins with real coefficients.

For example, we show in Fig. (9) the position probability distribution computed with initial coin state $\frac{1}{2}(|0\rangle + i|1\rangle)(|0\rangle + i|1\rangle)$. Fig. (9) bears a striking resemblance to those of Figs. (2 - 5). However, even though *qualita-*

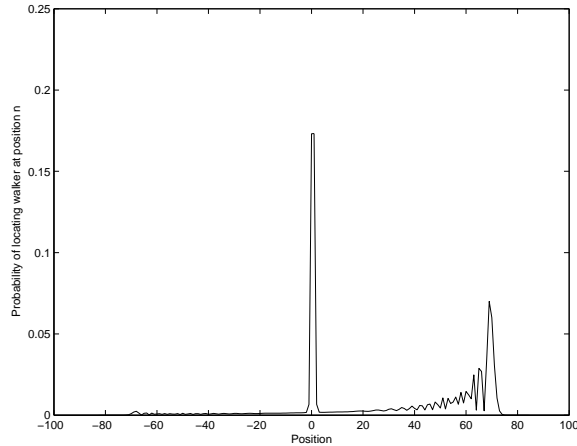


FIG. 7: Quantum walk computed with a coin initialized in the state $\frac{1}{2}(|0\rangle + |1\rangle)(|0\rangle + |1\rangle)$, i.e. a non-entangled state with real coefficients. 100 steps, coin and shift operators given by Eqs. (11) and (13) respectively.

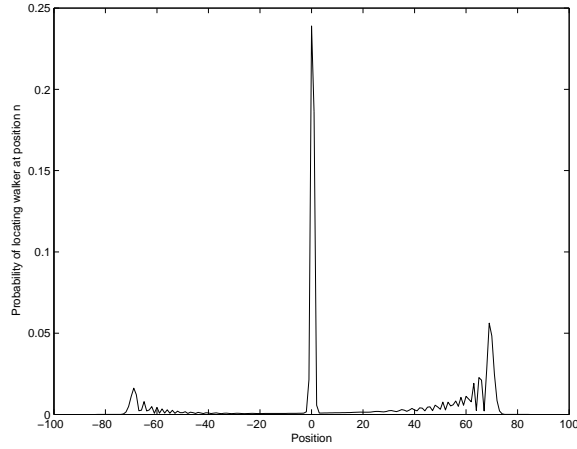


FIG. 8: Quantum walk computed with a coin initialized in the state $\frac{1}{2}|00\rangle + \frac{1}{2}|01\rangle + \frac{\sqrt{3}-1}{2}|10\rangle + \frac{\sqrt{3}+1}{2}|11\rangle$, i.e. a partially-entangled state with real coefficients. 100 steps, coin and shift operators given by Eqs. (11) and (13) respectively. Note that the entanglement of the coin initial state reduces the asymmetry of the graph by creating a new third peak.

tively a three peaked structure is evident, *quantitatively* it differs considerably. To illustrate this numerical difference, we appeal to Fig. (10), which compares three different quantum walks. The probability distribution computed with coin $\frac{1}{\sqrt{2}}(|00\rangle + |11\rangle)$ corresponds to the blue starred points on the graph, while the probability distributions computed with coins $\frac{1}{\sqrt{2}}(|00\rangle - |11\rangle)$ and $\frac{1}{2}|00\rangle + \frac{i}{2}|01\rangle + \frac{i}{2}|10\rangle - \frac{1}{2}|11\rangle$ are depicted using red dots and yellow circles respectively. Thus the entanglement of the initial coin state helps to both tune up and tune down the ratio of the central peak to the side peaks.

Numerical values show that entanglement plays an active role in the actual probability of finding the walker in a certain position. For example, consider walker po-

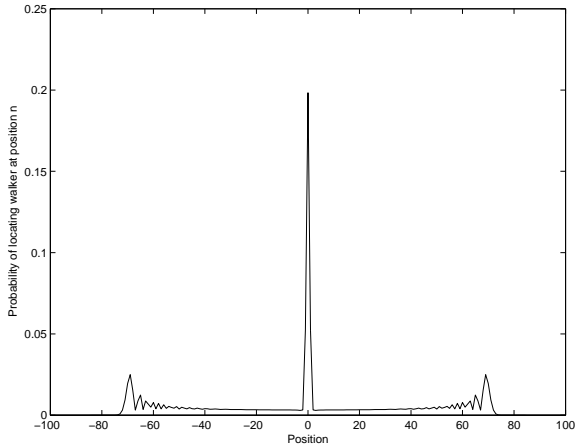


FIG. 9: Coin initial state is $\frac{1}{2}(|0\rangle + i|1\rangle)(|0\rangle + i|1\rangle)$. 100 steps, coin and shift operators given by Eqs. (11) and (13) respectively. The use of complex coefficients in the coin initial state delivers a symmetric probability distribution very similar to those shown in Figs.(2 - 5).

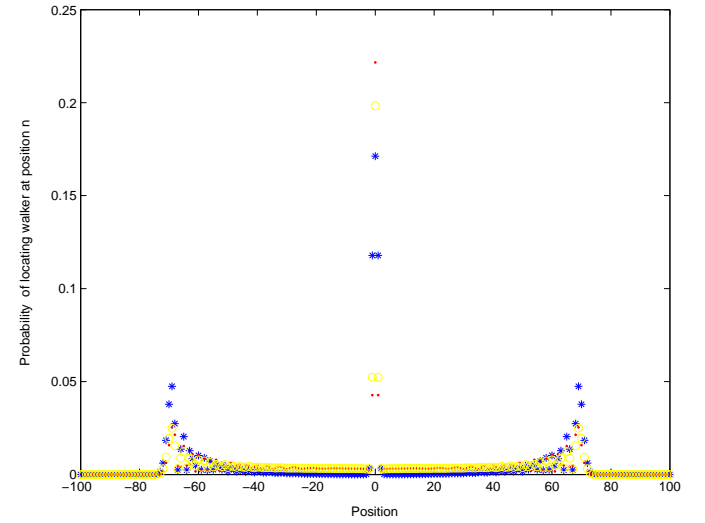


FIG. 10: The probability distribution computed with coin $\frac{1}{\sqrt{2}}(|00\rangle + |11\rangle)$ corresponds to the blue starred graph. Probability distributions computed with coins $\frac{1}{\sqrt{2}}(|00\rangle - |11\rangle)$ and $\frac{1}{2}|00\rangle + \frac{i}{2}|01\rangle + \frac{i}{2}|10\rangle - \frac{1}{2}|11\rangle$ are shown in red dots and yellow circles respectively. All graphs were computed after 100 steps using Eq. (11) as coin operator and Eq. (13) as shift operator.

sitions 60-70. The highest values in this region are attained by the probability distribution computed with coin $\frac{1}{\sqrt{2}}(|00\rangle + |11\rangle)$. In a different region, that of the central peak, the probability distribution of the non-entangled coin initial state $\frac{1}{2}|00\rangle + \frac{i}{2}|01\rangle + \frac{i}{2}|10\rangle - \frac{1}{2}|11\rangle$ is between those values produced by the two probability distributions obtained by computing quantum walks with maximally entangled states.

Another example of a symmetric graph produced using

coins in non-entangled states with complex coefficients has been presented by Inui and Konno in [46]. This symmetric graph was produced using a coin initialized in the state $\frac{i}{2}|00\rangle + \frac{i}{2}|01\rangle + \frac{1}{2}|10\rangle + \frac{1}{2}|11\rangle$.

V. QUANTUM WALKS WITH MORE THAN TWO MAXIMALLY ENTANGLED COINS

An interesting property of using several entangled qubits as coins is the fact that the number of coin and shift operators available for use also increases. Consequently, several different position probability distributions can be computed.

For example, in Fig.(11, red plot) the graph of a 100-steps quantum walk with the GHZ state $\frac{1}{\sqrt{2}}(|000\rangle + |111\rangle)$ as coin initial state is shown, the coin operator being given by $\hat{H}^{\otimes 3}$ where \hat{H} is Hadamard operator (Eq. (3)), and shift operator given by

$$\begin{aligned} \hat{S}_{3a} = & |000\rangle_{cc}\langle 000| \otimes \sum_i |i+1\rangle_{pp}\langle i| \\ & + |001\rangle_{cc}\langle 001| \otimes \sum_i |i\rangle_{pp}\langle i| \\ & + |010\rangle_{cc}\langle 010| \otimes \sum_i |i\rangle_{pp}\langle i| \\ & + |011\rangle_{cc}\langle 011| \otimes \sum_i |i\rangle_{pp}\langle i| \\ & + |100\rangle_{cc}\langle 100| \otimes \sum_i |i\rangle_{pp}\langle i| \\ & + |101\rangle_{cc}\langle 101| \otimes \sum_i |i\rangle_{pp}\langle i| \\ & + |110\rangle_{cc}\langle 110| \otimes \sum_i |i\rangle_{pp}\langle i| \\ & + |111\rangle_{cc}\langle 111| \otimes \sum_i |i-1\rangle_{pp}\langle i| \end{aligned} \quad (17)$$

which has a 4-peak probability distribution. However,

changing the shift operator to

$$\begin{aligned} \hat{S}_{3b} = & |000\rangle_{cc}\langle 000| \otimes \sum_i |i+3\rangle_{pp}\langle i| \\ & + |001\rangle_{cc}\langle 001| \otimes \sum_i |i+2\rangle_{pp}\langle i| \\ & + |010\rangle_{cc}\langle 010| \otimes \sum_i |i+1\rangle_{pp}\langle i| \\ & + |011\rangle_{cc}\langle 011| \otimes \sum_i |i\rangle_{pp}\langle i| \\ & + |100\rangle_{cc}\langle 100| \otimes \sum_i |i\rangle_{pp}\langle i| \\ & + |101\rangle_{cc}\langle 101| \otimes \sum_i |i-1\rangle_{pp}\langle i| \\ & + |110\rangle_{cc}\langle 110| \otimes \sum_i |i-2\rangle_{pp}\langle i| \\ & + |111\rangle_{cc}\langle 111| \otimes \sum_i |i-3\rangle_{pp}\langle i| \end{aligned} \quad (18)$$

results in the blue plot of Fig. (11) which has no such readily evident peak structure.

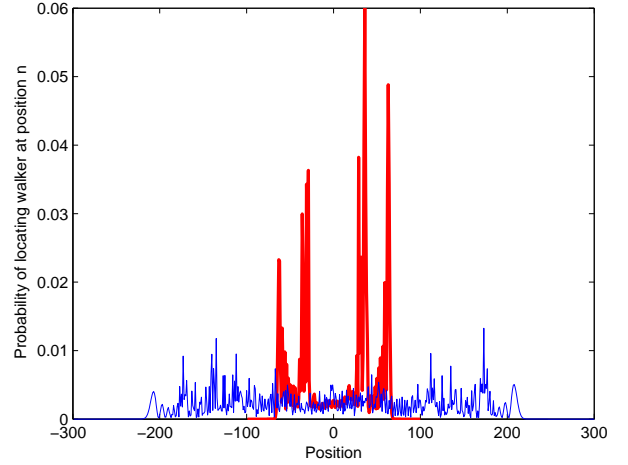


FIG. 11: Position probability distributions for two quantum walks on a line with GHZ state $\frac{1}{\sqrt{2}}(|000\rangle + |111\rangle)$ as initial tripartite coin state and coin operator $\hat{H}^{\otimes 3}$. The red plot was computed using the shift operator in Eq. (17) and the blue plot using the shift operator in Eq. (18). While the red plot shows an evident 4-peak structure, the blue plot does not present such a behaviour.

The potential richness of quantum walks increases when taking into consideration graphs of more than one dimension (efforts to understand the properties of quantum walks on graphs are presented in [13], while a proposal for a physical realization of a 2-dimensional quantum walk is given in [41]). For example, Fig. (12) shows the peak structure of a 50-step quantum walk on a graph with initial state given again by $\frac{1}{\sqrt{2}}(|000\rangle + |111\rangle)$, coin

operator given by $\hat{H}^{\otimes 3}$ and shift operator given by Eq. (19)

$$\begin{aligned}
 \hat{S}_{EC} = & |000\rangle_{cc}\langle 000| \otimes \sum_i |i+1, j\rangle_{pp}\langle i, j| \\
 & + |001\rangle_{cc}\langle 001| \otimes \sum_i |i, j\rangle_{pp}\langle i, j| \\
 & + |010\rangle_{cc}\langle 010| \otimes \sum_i |i, j+1\rangle_{pp}\langle i, j| \\
 & + |011\rangle_{cc}\langle 011| \otimes \sum_i |i, j\rangle_{pp}\langle i, j| \\
 & + |100\rangle_{cc}\langle 100| \otimes \sum_i |i, j\rangle_{pp}\langle i, j| \\
 & + |101\rangle_{cc}\langle 101| \otimes \sum_i |i, j-1\rangle_{pp}\langle i, j| \\
 & + |110\rangle_{cc}\langle 110| \otimes \sum_i |i, j\rangle_{pp}\langle i, j| \\
 & + |111\rangle_{cc}\langle 111| \otimes \sum_i |i-1, j\rangle_{pp}\langle i, j|
 \end{aligned} \tag{19}$$

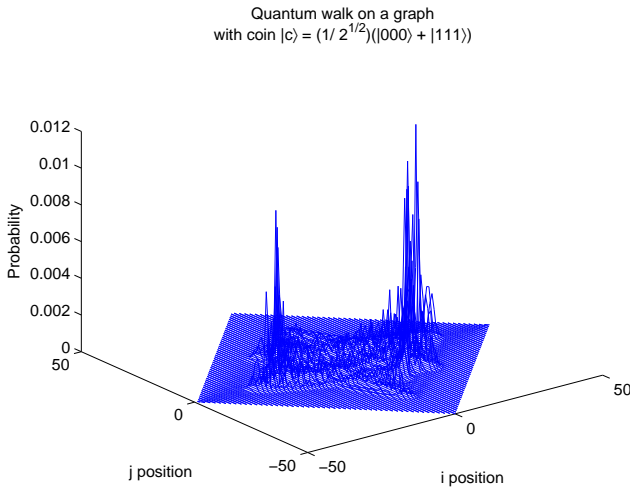


FIG. 12: Position probability distribution of a quantum walk on a 2-dimensional graph computed with coin initial state $\frac{1}{\sqrt{2}}(|000\rangle + |111\rangle)$ and shift operator given by Eq. (19). The number of steps is 50. The graph has 2 high peak regions and several other small peaks in the central region.

VI. CONCLUSIONS

We have studied quantum walks with maximally entangled coin initial states and have compared their behaviour with that of a classical random walk with a maximally correlated pair of coins as well as that of quantum walks with different degrees of entanglement. The probability distributions of such quantum walks have particular forms which are markedly different from the probability distributions of maximally correlated classical random walks. As for the single coin and entangled coins quantum walks, by changing the shift operator in the entangled case, one can generate a multitude of different probability distributions, some of which clearly differ from their single coin quantum walk counterparts.

The basic ‘three peak zone’ form is reproduced for a number of different entangled coin operators. In this case, the probability of finding the walker in the most likely position also appears to be higher when performing a quantum walk with a maximally entangled coin than when computing its classical counterpart (classical random walk with maximally correlated coin pair).

We have also considered how the ‘three peak zone’ form can also be produced by a quantum walk with coins using different initial conditions, i.e. a non-entangled coin with complex coefficients. Even though the shape of both probability distributions is similar, the quantum walks with maximally entangled coins have a different quantitative behaviour (higher or lower peaks, depending on the specific maximally entangled coin used). Entanglement allows symmetry in our probability distributions without using complex coefficients in initial coin states.

VII. ACKNOWLEDGMENTS

S.E. Venegas-Andraca gratefully acknowledges useful discussions with N. Paunković. This work was supported by CONACyT-México (scholarship 148528) and the UK Engineering and Physical Sciences Research Council.

- [1] R. Motwani and P. Raghavan, *Randomized Algorithms*. Cambridge University Press, 1995.
- [2] T. Hofmeister, U. Schöning, R. Schuler and O. Watanabe, “A Probabilistic 3-SAT Algorithm Further Improved”, 19th Symposium on Theoretical Aspects of Computer Science, pp. 192-202 (2002).
- [3] E. Farhi and S. Gutmann, Phys. Rev. A **58**, 915928 (1998).
- [4] C. Tamon, quant-ph/0209106.
- [5] A. Childs, E. Farhi, and S. Gutmann, Quantum Information Processing Vol. **1**, 35 (2002).
- [6] C. Moore and A. Russell, “Quantum Walks on the Hypercube”, In Proceedings of 6th International Workshop on Randomization and Approximation Techniques in Computer Science (RANDOM’02), Vol. 2483 of LNCS, pp. 164-178 (2002).

[7] H. Gerhardt and J. Watrous, "Continuous-Time Quantum Walks on the Symmetric Group", In Proceedings of 7th International Workshop on Randomization and Approximation Techniques in Computer Science (RANDOM'03), pp. 290-301 (2003).

[8] A. Ahmadi, R. Belk, C. Tamon, and C. Wendler, Quantum Information and Computation Vol. **3**, No. 6 pp. 611-618 (2003).

[9] Fedichkin L, Solev D and Tamon D, "Mixing and decoherence in continuous-time quantum walks on cycles", quant-ph/0509163

[10] Y. Aharonov, L. Davidovich, and N. Zagury, Phys. Rev. A **48**, pp. 1687-1690 (1993).

[11] D.A. Meyer, J. Stat. Phys. **85**, pp. 551-574 (1996).

[12] A. Nayak and A. Vishwanath, quant-ph/0010117.

[13] D. Aharonov, A. Ambainis, J. Kempe, and U. Vazirani, "Quantum Walks on Graphs", In Proceedings of the 33th ACM Symposium on The Theory of Computing (STOC'01), pp.50-59 (2001).

[14] T.A. Brun, H.A. Carteret, and A. Ambainis, Phys. Rev. Lett. **91**, 130602 (2003).

[15] H. Jeong, M. Paternostro and M.S. Kim, Phys. Rev. A **69**, 012310 (2004).

[16] P.L. Knight, E. Roldán, and J.E. Sipe, J. Mod. Op. Vol. **51**, No. 12, pp. 1761-1777 (2004).

[17] A. Ambainis, E. Bach, A. Nayak, A. Vishwanath, and J. Watrous, "One-dimensional Quantum Walks", In Proceedings 33th STOC-ACM, pp.60-69 (2001).

[18] J. Kempe, "Discrete Quantum Walks Hit Exponentially Faster", In Proceedings of 7th International Workshop on Randomization and Approximation Techniques in Computer Science (RANDOM'03), pp. 354-369 (2003).

[19] N. Shenvi, J. Kempe, and K.B. Whaley, Phys. Rev. A **67** (5), 052307 (2003).

[20] A.M. Childs, R. Cleve, E. Deotto, E. Farhi, S. Gutmann, and D. Spielman, "Exponential Algorithmic Speedup by Quantum Walk", In Proceedings of the 35th ACM Symposium on The Theory of Computation (STOC'03), pp. 59-68 (2003).

[21] A. Ambainis, "Quantum walk algorithm for element distinctness", In Proceedings of 45th Annual IEEE Symposium on Foundations of Computer Science (FOCS'04) pp. 22-31 (2004).

[22] J. Kempe, Contemporary Physics Vol. 44 (4), pp.307-327 (2003).

[23] A. Ambainis, "Quantum Walks and their algorithmic applications", International Journal of Quantum Information Vol. **1** No. 4 pp. 507-518 (2003).

[24] T.A. Brun, H.A. Carteret, and A. Ambainis, Phys. Rev. A **67**, 052317 (2003).

[25] B. Tregenna, W. Flanagan, R. Maile, and V. Kendon, New J. Phys. **5** 83 (2003).

[26] A. Ambainis, J. Kempe, and A. Rivosh, "Coins Make Quantum Walks Faster", To appear in Proc. 16th ACM-SIAM SODA pp 1099-1108 (2005), quant-ph/0402107.

[27] V. Kendon and B. Tregenna, Phys. Rev. A **67**, 042315 (2003).

[28] V. Kendon and B. Tregenna, "Decoherence in Discrete Quantum Walks", Selected Lectures from DICE 2002. Lecture Notes in Physics **633**, pp. 253-267 (2003)

[29] T.A. Brun, H.A. Carteret, and A. Ambainis, Phys. Rev. A **67**, 032304 (2003).

[30] J. Du, H. Li, X. Xu, M. Shi, J. Wu, X. Zhou and R. Han, Phys. Rev. A **67** 042316 (2003), quant-ph/0203120.

[31] I. Carneiro, M. Loo, X. Xu, M. Girerd, V. Kendon and P. Knight, New J. Phys. **7** (2005) 156

[32] J. Endrejat and H. Buttner, quant-ph/0507184.

[33] G. Abal, R. Siri, A. Romanelli and R. Donangelo, quant-ph/0507264.

[34] Y. Omar, N. Paunković, L. Sheridan, and S. Bose, quant-ph/0411065.

[35] T.D. MacKay, S.D. Bartlett, L.T. Stephenson and B.C. Sanders, "Quantum walks in higher dimensions", J. Phys. A. (Math. Gen.) **35**, pp. 2745-2753 (2002).

[36] G. Grimmett and D. Welsh, *Probability: an introduction*. Oxford University Press, 1991.

[37] C. H. Bennett, H. J. Bernstein, S. Popescu and B. Schumacher, Phys. Rev. A **53**, 2046 (1996).

[38] U. Schöning, "A Probabilistic Algorithm for k-SAT and Constraint Satisfaction Problems", Proc. IEEE Symposium on Foundations of Computer Science, pp. 410-414, (1999).

[39] E. Bach, S. Coppersmith, M. Paz Goldshen, R. Joynt and J. Watrous, Journal of Computer and Systems Sciences **69**(4) pp. 562 – 592 (2004)

[40] T. Yamasaki, H. Kobayashi and H. Imai, Phys. Rev. A **68**, 012302 (2003)

[41] E. Roldán and J.C. Soriano, quant-ph/0503069.

[42] B. C. Sanders, S. D. Bartlett, B. Tregenna and P. L. Knight, Phys. Rev. A **67**, 042305 (2003).

[43] B. C. Travaglione and G. J. Milburn, Phys. Rev. A **65**, 032310 (2002).

[44] M. A. Rowe, D. Kielpinski, V. Meyer, C. A. Sacket, W. M. Itano, C. Monroe and D. J. Wineland, Nature **409**, pp 791-794 (2001).

[45] M.B. Plenio, S.F. Huelga, A. Beige, P.L. Knight, Phys. Rev. A **59**, 2468-2475 (1999).

[46] N. Inui and N. Konno, "Localization of multi-state Quantum Walk in One Dimension", Phys. A **(353)** pp 133-144 (2005), quant-ph/0403153.